plasma is encountered. In this region, the flowing plasma is observed simply as an energetic ion current level, which on some orbits is observed to extend outward for thousands of kilometers beyond the ionopause to the bow shock, and is attributed to shocked solar wind plasma. In the region of the shaded portion of Fig. 4 and higher in the energetic plasma region, the profiles shown for O^+, O_2^+, and N^+ are not directly representative of thermal ion concentrations, and require further analysis.

Additional observations of dynamic response are indicated within the ion composition results. Some features not necessarily associated with the solar wind interaction include tentative evidence of (i) an apparent increase in the ratio He^+/H^+ approaching the terminator, which may reflect transport of He to the nightside, and (ii) a stratification signature in the lower ionosphere which may identify the location of the exobase. With the increasing body of data becoming available, we anticipate the opportunity to obtain a detailed picture of dynamic responses throughout the ionosphere of Venus.

HARRY A. TAYLOR, JR.
HENRY C. BRINTON
SIEGFRIED J. BAUER
RICHARD E. HARTLE
NASA/Goddard Space Flight Center, Greenbelt, Maryland 20771
PAUL A. CLOUTIER, F. CURTIS MICHEL
ROBERT E. DANIELL, JR.
Rice University, Houston, Texas 77001
THOMAS M. DONAHUE
University of Michigan, Ann Arbor
RONALD C. MAEHL
Norlin Communications, Inc., College Park, Maryland 20740

References and Notes

1. H. A. Taylor, H. C. Brinton, S. J. Bauer, R. E. Hartle, T. M. Donahue, P. A. Cloutier, F. C. Michel, R. E. Daniell, Jr., B. H. Blackwell, *Science* **203**, 752 (1979).
2. L. Colin and D. M. Hunten, *Space Sci. Rev.* **20**, 458 (1977).
3. N. F. Ness, K. W. Behannon, R. P. Lepping, Y. C. Whang, K. H. Schatten, *Science* **183**, 1301 (1974).
4. S. J. Bauer and R. E. Hartle, *Geophys. Res. Lett.* **1**, 7 (1974).
5. H. A. Taylor, Jr., H. C. Brinton, M. W. Pharo III, *J. Geophys. Res.* **73**, (1968).
6. S. J. Bauer, in *NASA Spec. Publ. SP-397* (1976), p. 47.
7. J. Wolfe, D. S. Intriligator, J. Mihalov, H. Collard, D. McKibbin, R. Whitten, A. Barnes, *Science* **203**, 750 (1979).
8. P. A. Cloutier and R. E. Daniell, Jr., *Planet. Space Sci.* **21**, 463 (1973); R. E. Daniell, Jr., and P.A. Cloutier, *ibid.* **25**, 621 (1977).
9. P. A. Cloutier *et al.*, *ibid.* **22**, 967 (1974).
10. We thank those who contributed to make this experiment possible, in particular J. Burcham, M. Pharo, and T. Page of Goddard Space Flight Center, G. Cordier, T. C. G. Wagner, D. Simons, J. Larsen, D. Tallon, P. Lepanto, and R. Scelsi of Norlin Communications, Inc., J. Coulson of Ideas, Inc., and M. Heffernan of CSTA, Inc. We also thank L. Colin for reviewing the manuscript.

15 January 1979

Thermal Structure and Major Ion Composition of the Venus Ionosphere: First RPA Results from Venus Orbiter

Abstract. *Thermal plasma quantities measured by the retarding potential analyzer (RPA) are, together with companion Pioneer Venus measurements, the first in situ measurements of the Venus ionosphere. High ionospheric ion and electron temperatures imply significant solar wind heating of the ionosphere. Comparison of the measured altitude profiles of the dominant ions with an initial model indicates that the ionosphere is close to diffusive equilibrium. The ionopause height was observed to vary from 400 to 1000 kilometers in early orbits. The ionospheric particle pressure at the ionopause is apparently balanced at a solar zenith angle of about 70° by the magnetic field pressure with little contribution from energetic solar wind particles. The measured ratio of ionospheric scale height to ionopause radius is consistent with that inferred from previously measured bow shock positions.*

The Pioneer Venus orbiter was inserted into a highly eccentric orbit on 4 December 1978, with an apoapsis of 66,000 km (*1*). Every 24 hours the spacecraft passes into the ionosphere for approximately 10 minutes, during which time the following data were obtained.

The primary ionospheric quantities, ion temperature (T_i), total and major ion concentrations, ion bulk velocity, electron temperature (T_e), and suprathermal electron energy distribution, are being

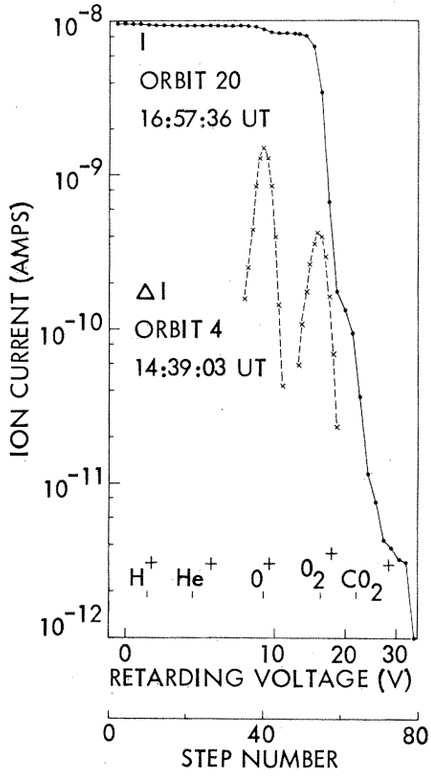

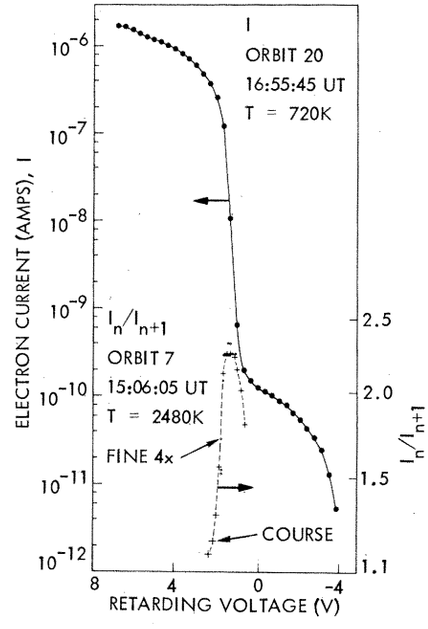

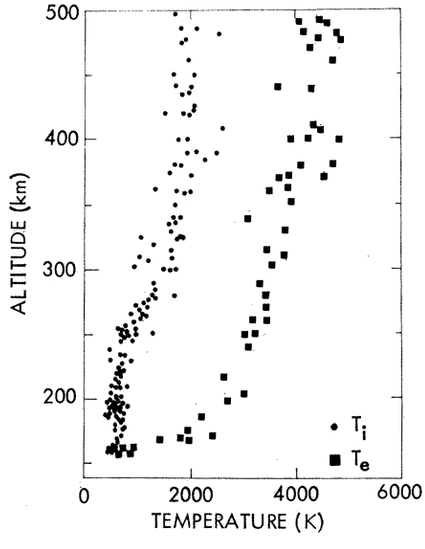

Fig. 1 (above). Ion-retarding curve *I* during orbit 20 indicating O^+, O_2^+, and CO_2^+ as dominant ions; current differences between successive steps ΔI during orbit 4 showing the two dominant ion species O^+ and O_2^+. Fig. 2 (top right). Complete electron retarding curve *I* transmitted during orbit 20 and current ratios from successive steps I_n/I_{n+1} around the strongest decrease of the semilogarithmic characteristic during orbit 7 near periapsis. Fig. 3 (bottom right). Electron temperature (T_e) and ion temperature (T_i) profiles measured during six of the first ten orbits.

0036-8075/79/0223-0757$00.50/0

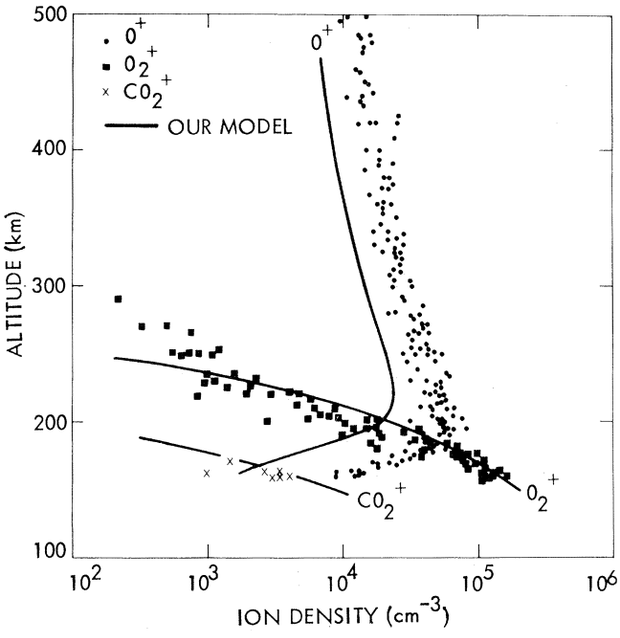

Fig. 4. Major ion composition measured during six of the first ten orbits compared with our model density.

measured by a retarding potential analyzer (RPA) specifically designed for a low telemetry rate (*2*). Figure 1 illustrates a complete ion current-voltage (*I-V*) curve returned in the diagnostic RPA mode and ΔI values between successive steps selected around two major ion peaks and returned in the peak RPA mode. Ion concentration, temperature, and mass are determined, respectively, by the peak current difference, half width, and step number. Figure 2 illustrates a complete electron *I-V* curve returned in a diagnostic RPA mode of operation and an example of successive values of the electron current ratio ($\Delta \log I$) selected by the RPA logic around the exponentially varying portion of the *I-V* curve and returned in the telemetry-economic peak RPA mode. The electron temperature is inversely proportional to $\Delta \log I / \Delta V$. The RPA was operated largely in the peak mode in order to ensure economic use of the available telemetry rate.

The results presented are believed to represent the typical or usual condition of the ionosphere during the first ten orbits. Solar zenith angles (SZA) represented are 65° to 80°. Ion bulk velocity and suprathermal electron energy distribution data will be reported in later papers.

Ion and electron temperatures. Typical values of T_i and T_e at an altitude of 500 km are 2000 and 4500 K, respectively, and vary only slowly with altitude above 400 km (Fig. 3). Although we have shown data only to 500 km, this statement holds to the ionopause altitude. Heating by the solar wind is apparently required to produce comparable temperatures in ionospheric models (*3*, *4*). The value of T_i is approximately constant between 250 and 160 km; T_e decreases rapidly in the lower altitude range and has almost reached T_i at 160 km.

Major ion composition. The major ion above 180 km is O^+, and it comprises more than 90 percent of the concentration between 220 km and the ionopause (Fig. 4). Light ion peaks H^+ and He^+ were only occasionally detected by the RPA logic, but the full *I-V* curves and the occasionally selected peaks indicate that the light ion concentration approaches 10 percent of the total on occasion. The most abundant ion below 180 km is O_2^+; CO_2^+ is just becoming detectable by the RPA below 180 km.

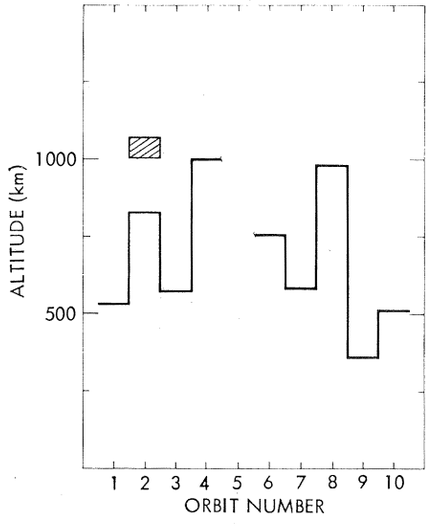

Fig. 5. Height of the ionopause inferred from thermal ion measurements averaged over the inbound and outbound legs.

Ionopause altitude. The ionospheric thermal plasma density drops rapidly from $\sim 1 \times 10^4$ cm^{-3} to very low values at the ionopause. The ionopause altitude measured on the first ten orbits is shown in Fig. 5. We define the ionopause as the level above which the ionospheric concentration first drops below $\simeq 100$ cm^{-3}. The altitude was usually about the same inbound and outbound on a single orbit but varied strongly from orbit to orbit. The spacecraft occasionally moved through detached patches of lower-density plasma or through spatial irregularities in ionopause height (as indicated by the stippled area above the ionopause for orbit 2 in Fig. 5).

Preliminary interpretation. Our initial ionospheric modeling efforts are indicated by the curves in Fig. 4. The model is similar in most respects to that of Chen and Nagy (*4*). Ion and electron number densities are computed by solving the appropriate conservation equations which include the motion of O^+, H^+, and He^+. Other ions are held in chemical equilibrium. The ion O^+ was assumed to be in diffusive equilibrium at the upper boundary. We included distributed contributions to the ion and electron heating by the solar wind, which were equivalent to $\sim 2 \times 10^8$ and $\sim 4 \times 10^{10}$ eV cm^{-2} sec^{-1}, respectively, inserted at the ionopause. The model atmosphere had a thermospheric temperature of 350 K and number densities at 200 km similar to those assumed by Chen and Nagy: $[CO_2] = 1 \times 10^7$ cm^{-3}, $[O] = 10^8$ cm^{-3}. The solar extreme-ultraviolet fluxes are those given by Hinteregger (*5*).

The following tentative conclusions can be drawn from a comparison of the model results with observation: O^+ ions appear close to diffusive equilibrium above 220 km; O_2^+ goes into diffusive equilibrium above $\sim$ 230 km, and strong heating of the ionosphere, apparently by the solar wind, is required to explain the temperature profiles. The small overestimate of the CO_2^+ and O_2^+ abundances and the overestimate of the height of the O^+ concentration peak suggest that the abundance of neutral O was underestimated and the abundance of neutral CO_2 overestimated.

Solar wind–planetary interaction. An important parameter in the interaction of the solar wind with the Venus ionosphere is the ratio of ionosphere scale height (H) to the radius (r_0) of the ionopause at the subsolar point (*6*). Using either values of the measured ion mass, T_e, and T_i at 500-km altitude, or the directly

observed decrease of O^+ with altitude, we obtain at SZA = 70° the value H/r_0 " 0.07. The quantity H, and consequently H/r_0, are approximately constant above 400 km. The ratio of 0.07 derived from measured parameters lies midway in the range of values that have been inferred from measurements of the shock position (*6*, *7*).

Pressure balance across the ionopause. If we assume that under steady conditions the magnetic field in the vicinity of the ionopause is tangent to the ionopause, we may expect the expression $(B^2/8\pi + p)$ to remain constant as the boundary is traversed (*6*, *8*) (B is the local magnetic field strength, and P is the local charged particle pressure). The typical particle pressure at 500 km may be evaluated from Figs. 3 and 4. Inside the ionosphere B is typically (but with significant exceptions) of the order of 1 γ (*9*). Using these values to evaluate the expression in the ionosphere and normalizing, we obtain:

$$\left|\left(\frac{B}{48\ \gamma}\right)^2 + \left(\frac{n}{10^4\ \mathrm{cm}^{-3}}\right)\left(\frac{T_e + T_i}{6500\ \mathrm{K}}\right)\right| \doteq 1 \quad (1)$$

where n is the local plasma density. In passing into the ionopause from below, the thermal concentration decreases toward 10 cm^{-3} and T_e and T_i remain approximately constant. If we assume that no high-temperature particles are present in the boundary region, Eq. 1 requires B to be 48 γ. Russell (*9*) reports that for most of the early orbits B increases to 40 to 60 γ at the ionopause. The magnetic field is typically supplying the bulk of the pressure balance, which implies that particles with shocked solar wind energy do not contribute significantly to the balance at the ionopause at SZA = 70°.

W. C. KNUDSEN
Lockheed Palo Alto Research Laboratory, Palo Alto, California 94304
K. SPENNER
Institut für Physikalische Weltraumsforschung der Fraunhofer Gesellschaft, 78 Freiburg, West Germany
R. C. WHITTEN
NASA Ames Research Center Moffet Field, California 94035
J. R. SPREITER
Stanford University, Stanford, California 94305
K. L. MILLER
Lockheed Palo Alto Research Laboratory
V. NOVAK
Institut für Physikalische Weltraumsforschung der Fraunhofer Gesellschaft

References and Notes

1. L. Colin and C. F. Hall, *Space Sci. Rev.* **20**, 283 (1977).
2. W. C. Knudsen, J. Bakke, K. Spenner, V. Novak, *Space Sci. Instrum.*, in press.
3. R. C. Whitten, *J. Geophys. Res.* **74**, 5623 (1969).
4. R. H. Chen and A. F. Nagy, *ibid.* **83**, 1133 (1978).
5. H. E. Hinteregger, *J. Atmos. Terr. Phys.* **38**, 791 (1976).
6. J. R. Spreiter, A. L. Summers, A. W. Rizzi, *Planet. Space Sci.* **18**, 1281 (1970).
7. C. T. Russell, in *Solar System Plasma Physics*, C. F. Kennel, L. J. Lanzerotti, E. N. Parker, Eds. (North-Holland, New York, in press).
8. C. L. Longmire, *Elementary Plasma Physics* (Interscience, New York, 1963).
9. C. T. Russell, R. C. Elphic, J. A. Slavin, *Science* **203**, 745 (1979).

10. The RPA experiment is supported by NASA through contract NAS2-9481 and by Bundesminister für Forschung and Technologie through contract 01 Do 238 (RV 14-B 28/73). We thank all those whose dedicated efforts made possible the perfectly working RPA.

16 January 1979

Electron Temperatures and Densities in the Venus Ionosphere: Pioneer Venus Orbiter Electron Temperature Probe Results

Abstract. *Altitude profiles of electron temperature and density in the ionosphere of Venus have been obtained by the Pioneer Venus orbiter electron temperature probe. Elevated temperatures observed at times of low solar wind flux exhibit height profiles that are consistent with a model in which less than 5 percent of the solar wind energy is deposited at the ionopause and is conducted downward through an unmagnetized ionosphere to the region below 200 kilometers where electron cooling to the neutral atmosphere proceeds rapidly. When solar wind fluxes are higher, the electron temperatures and densities are highly structured and the ionopause moves to lower altitudes. The ionopause height in the late afternoon sector observed thus far varies so widely from day to day that any height variation with solar zenith angle is not apparent in the observations. In the neighborhood of the ionopause, measurements of plasma temperatures and densities and magnetic field strength indicate that an induced magnetic barrier plays an important role in the pressure transfer between the solar wind and the ionosphere. The bow shock is marked by a distinct increase in electron current collected by the instrument, a feature that provides a convenient identification of the bow shock location.*

The Pioneer Venus orbiter electron temperature probe (OETP) is designed to measure the thermal structure of the ionosphere of Venus. These data should permit us to better understand the processes by which the ionosphere is heated and cooled. The case of Venus is of particular interest in this regard because of the strong interaction expected between the solar wind and the ionosphere of this weakly magnetized planet. Unlike Earth and Jupiter, whose strong

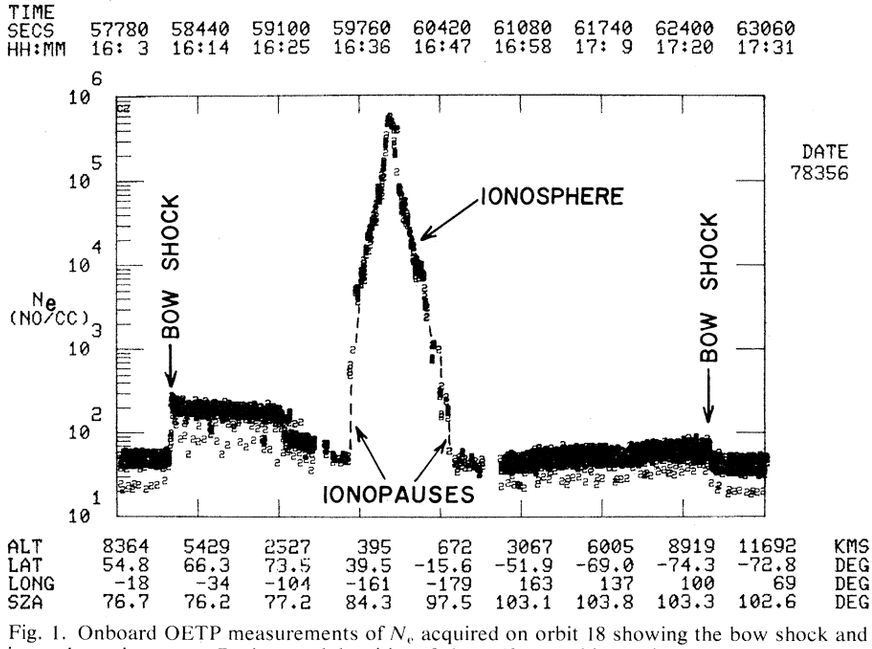

Fig. 1. Onboard OETP measurements of N_e acquired on orbit 18 showing the bow shock and ionosphere signatures. Background densities of about 50 per cubic centimeter are due to spacecraft photoelectrons.

0036-8075/79/0223-0763$00.50/0